

# Refinement of the Crystal Structures of Palladium-rich In-Pd Compounds by X-Ray and Neutron Powder Diffraction

Holger Kohlmann<sup>a</sup> and Clemens Ritter<sup>b</sup>

<sup>a</sup> FR. 8.1 Anorganische und Analytische Chemie und Radiochemie, Universität des Saarlandes, Postfach 15 11 50, 66041 Saarbrücken, Germany

<sup>b</sup> Institut Laue-Langevin, 6, Rue Jules Horowitz, BP 156, 38042 Grenoble Cedex 9, France

Reprint requests to Dr. H. Kohlmann. Tel.: +49 681 302 3378. Fax: +49 681 302 4233.

E-mail: h.kohlmann@mx.uni-saarland.de

*Z. Naturforsch.* **2007**, *62b*, 929–934; received March 3, 2007

*Dedicated to Dr. Bernard Chevalier on the occasion of his 60<sup>th</sup> birthday*

The ternary indium palladium intermetallics  $\text{In}_3\text{Pd}_5$ ,  $\text{InPd}_2$ , and  $\text{InPd}_3$  have been synthesized by iodine-catalyzed reactions from the elements. Rietveld refinements on X-ray powder diffraction patterns provide the first accurate crystal structure data for  $\text{In}_3\text{Pd}_5$  (*Pbam*, No. 55,  $a = 1104.20(2)$ ,  $b = 561.346(8)$ ,  $c = 424.263(6)$  pm,  $\text{Rh}_5\text{Ge}_3$ -type) and  $\text{InPd}_2$  (*Pnma*, No. 62,  $a = 561.676(6)$ ,  $b = 421.710(4)$ ,  $c = 822.78(8)$  pm,  $\text{Co}_2\text{Si}$ -type). X-Ray powder diffraction apparently confirms the  $\text{TiAl}_3$  structure type proposed in the literature for  $\text{InPd}_3$ . However, Rietveld refinement on neutron powder diffraction data reveals an In/Pd distributional disorder. Therefore, we describe the crystal structure of  $\text{InPd}_3$  in a AuCu-type model instead (*P4/mmm*, No. 123,  $a = 287.224(4)$ ,  $c = 380.079(7)$  pm), with mixed occupancy of one crystallographic site by 50 % In and 50 % Pd. In contrast to  $\text{In}_3\text{Pd}_5$  and  $\text{InPd}_2$ , which can be considered to be line compounds,  $\text{InPd}_3$  shows a non-negligible homogeneity range with unit cell volumes ranging from  $0.126132(5)$  nm<sup>3</sup> for the indium-rich to  $0.125474(8)$  nm<sup>3</sup> for the palladium-rich  $\text{In}_{1+x}\text{Pd}_{3-x}$  phases. Mean In–Pd distances in these indium palladium intermetallics range from 272.3 pm (In1 in  $\text{In}_3\text{Pd}_5$ ) with coordination number 8 for indium to 281.2 pm for 12-coordinated In in  $\text{InPd}_3$ .

**Key words:** Intermetallic Compounds, Palladium, Neutron Diffraction, Powder Diffraction, Disorder

## Introduction

Various approaches have been used to influence crystal structures and physical properties of intermetallic compounds, as, *e. g.*, high pressure and isotopic substitution [1–3]. A further strategy is the incorporation of hydrogen for tuning the magnetic behaviour of intermetallic compounds of the transition metals [4, 5], and more recently in the group of Chevalier for probing mixed-valent and heavy fermion behaviour of intermetallics with cerium and elements of the groups 8–10 ([6–16] and references cited therein).

The metal hydrides of intermetallic compounds  $M_mM'_{m'}$  ( $M' = \text{Fe, Co, Ni, Ru, Rh, Pd, Os, Ir, Pt}$ ) reveal a fascinating structural chemistry [17], including unusual coordination geometries [18], high oxidation states [19, 20], and order-disorder transitions [21, 22]. Ternary palladium hydrides with divalent metals exhibit a wide variety of chemical bonding, crystal struc-

tures and properties, ranging from ionic-covalent complex hydrides to typical interstitial compounds with metallic properties, as, *e. g.*, in the systems Ca-Pd-H [23, 24], Sr-Pd-H [25, 26], and Eu-Pd-H [27]. A particularly interesting example of the subtle influence of hydrogen on the crystal structure of intermetallics is formed upon hydrogenation of  $\text{MgPd}_3$ . Here, a hydrogen-induced rearrangement of metal atoms from a  $\text{ZrAl}_3$  to a  $\text{AuCu}_3$  structure has been found [28]. As these structures are closely related, they can easily be mistaken one for the other, especially in the case of incomplete order. Therefore, detailed studies require a precise knowledge of the crystal structures of the intermetallic compounds underlying the metal hydrides. In an extension of our work on palladium-rich intermetallics and hydrides, we report in this paper on the refinement of the crystal structures of the palladium-rich phases  $\text{In}_3\text{Pd}_5$ ,  $\text{InPd}_2$  and  $\text{InPd}_3$ , which are interesting candidates for hydrogenation studies.

<b>In<sub>3</sub>Pd<sub>5</sub></b> : <i>Pbam</i> (No. 55), $a = 1104.20(2)$ , $b = 561.346(8)$ , $c = 424.263(6)$ pm					
$R_p = 0.019$ , $R_{wp} = 0.028$ , $R'_p = 0.150$ , $R'_{wp} = 0.113$ , $R_{Bragg} = 0.042$ , $S = 1.02$					
atom site	$x$	$y$	$z$	$B_{iso}$ ( $10^4$ pm <sup>2</sup> )	
In1	2a	0	0	1.4(1)	
In2	4h	0.1428(2)	0.3273(4)	1/2	1.59(9)
Pd1	2c	0	1/2	0	0.8(1)
Pd2	4g	0.2443(2)	0.0735(4)	0	0.70(8)
Pd3	4h	0.3915(2)	0.3018(5)	1/2	0.47(8)
<b>InPd<sub>2</sub></b> : <i>Pnma</i> (No. 62), $a = 561.676(6)$ , $b = 421.710(4)$ , $c = 822.78(8)$ pm					
$R_p = 0.020$ , $R_{wp} = 0.029$ , $R'_p = 0.173$ , $R'_{wp} = 0.118$ , $R_{Bragg} = 0.039$ , $S = 1.11$					
atom site	$x$	$y$	$z$	$B_{iso}$ ( $10^4$ pm <sup>2</sup> )	
In	4c	0.8222(3)	1/4	0.3989(2)	1.20(5)
Pd1	4c	0.8400(3)	1/4	0.0723(2)	1.15(5)
Pd2	4c	0.9329(3)	1/4	0.7318(2)	0.89(4)
<b>InPd<sub>3</sub></b> : <i>P4/mmm</i> (No. 123), $a = 287.224$ (4), $c = 380.079$ (7) pm					
$R_p = 0.060$ , $R_{wp} = 0.083$ , $R'_p = 0.154$ , $R'_{wp} = 0.137$ , $R_{Bragg} = 0.030$ , $S = 5.33$					
atom site	$x$	$y$	$z$	$B_{iso}$ ( $10^4$ pm <sup>2</sup> )	occupancy
In1	1a	0	0	0.43(5)	0.5
Pd1	1a	0	0	$B_{iso}$ (In1)	0.5
Pd2	1d	1/2	1/2	0.51(4)	1.0

## Experimental Section

### Synthesis

Indium palladium intermetallic compounds have been prepared from the elements in evacuated sealed silica tubes in analogy to the iodine-catalyzed synthesis, as applied previously in the systems Al-Pd, Ga-Pd, Be-Pd, and Mg-Pd [29–32]. Indium pieces (99.99%, Schuchard, Munich) and palladium powder (< 60  $\mu$ m, 99.9%, ChemPur) in stoichiometric ratios, and iodine (Merck, purified by sublimation) with molar ratios ranging from 0.5 to 2% with respect to indium have been used. The silica ampoules were heated with 50 K h<sup>-1</sup> to 850 K, annealed at this temperature for 55 h and quenched in air. Iodine was sublimed off the products by gently heating one end of the sealed silica tube. For synthesis temperatures substantially below 850 K incomplete reactions were observed, yielding multiphasic mixtures. In the case of InPd<sub>3</sub>, reaction at 750 K produced a mixture of two phases of the approximate composition InPd<sub>3</sub> with slightly different unit cell volumes.

### Powder diffraction and Rietveld refinement

X-Ray powder diffraction data were collected using flat transmission samples containing an internal silicon standard on an image plate Guinier powder diffractometer (Huber Guinier camera G670 at  $T = 296(1)$  K with  $CuK\alpha_1$  radiation,  $\lambda = 154.056$  pm). Rietveld refinements were carried out using the program FULLPROF [33] with a pseudo-Voigt profile function in all cases. For the refinement of In<sub>3</sub>Pd<sub>5</sub> on X-ray powder data the following parameters were allowed to vary: the zero point of the  $2\theta$  scale, one scale parameter, three peak width ( $u$ ,  $v$ ,  $w$  of the Cagliotti formula), one mixing ( $\eta$ ), two asymmetry and one isotropic displacement parameters for the internal silicon standard, keeping its lattice parameter fixed at 543.0 pm; one scale parameter, three peak

width ( $u$ ,  $v$ ,  $w$  of the Cagliotti formula), one mixing ( $\eta$ ), two asymmetry, three lattice, six positional and five isotropic displacement parameters for the main In<sub>3</sub>Pd<sub>5</sub> phase; one scale and three lattice parameters for the minor phase InPd<sub>2</sub> with all profile parameters constrained to those of the main In<sub>3</sub>Pd<sub>5</sub> phase. The background was described by linear interpolation between 28 points. A similar strategy was chosen for the refinement on the InPd<sub>2</sub> X-ray powder data. Silicon was treated in exactly the same way as described before, and the main phase InPd<sub>2</sub> as well, except for a reduced number of three isotropic displacement parameters. For the minor phase InPd<sub>3</sub> one scale parameter, one peak width ( $w$  of the Cagliotti formula), one lattice and one overall isotropic displacement parameters were refined, and the background was described by linear interpolation between 24 points.

<sup>a</sup> Definition of  $R$  factors:  $R_p = \sum |y_i(\text{obs}) - y_i(\text{calc})| / \sum y_i(\text{obs})$ ;  $R_{wp} = [ \sum w_i (y_i(\text{obs}) - y_i(\text{calc}))^2 / \sum w_i y_i(\text{obs})^2 ]^{1/2}$ ;  $R'_p$  and  $R'_{wp}$  are calculated as above but using background-corrected counts;  $R_{Bragg} = \sum |I_B(\text{'obs'}) - I_B(\text{calc})| / \sum I_B(\text{'obs'})$ . Form of the temperature factor:  $\exp[-B_{iso}(\sin \theta / \lambda)^2]$ .

width ( $u$ ,  $v$ ,  $w$  of the Cagliotti formula), one mixing ( $\eta$ ), two asymmetry, three lattice, six positional and five isotropic displacement parameters for the main In<sub>3</sub>Pd<sub>5</sub> phase; one scale and three lattice parameters for the minor phase InPd<sub>2</sub> with all profile parameters constrained to those of the main In<sub>3</sub>Pd<sub>5</sub> phase. The background was described by linear interpolation between 28 points. A similar strategy was chosen for the refinement on the InPd<sub>2</sub> X-ray powder data. Silicon was treated in exactly the same way as described before, and the main phase InPd<sub>2</sub> as well, except for a reduced number of three isotropic displacement parameters. For the minor phase InPd<sub>3</sub> one scale parameter, one peak width ( $w$  of the Cagliotti formula), one lattice and one overall isotropic displacement parameters were refined, and the background was described by linear interpolation between 24 points.

Neutron powder diffraction data on InPd<sub>3</sub> were taken at  $T = 299(2)$  K on the high-resolution powder diffractometer D1A at the Institute Laue-Langevin in Grenoble, France, in the range  $6^\circ \leq 2\theta \leq 157^\circ$  (step size  $\Delta 2\theta = 0.05^\circ$ ) during a total measurement time of 12 h. Special care was taken of the enhanced neutron absorption of indium by realizing a moderate sample thickness (3.8 g InPd<sub>3</sub> powder in a vanadium can of 5 mm inner diameter, sealed by indium wire). The wavelength used was determined from a measurement on a silicon standard to be  $\lambda = 190.931(3)$  pm and kept fixed during refinements. For the refinement on InPd<sub>3</sub> neutron powder data the following parameters were allowed to vary: the zero point of the  $2\theta$  scale, five background parameters (polynomial), one scale, three peak width ( $u$ ,  $v$ ,  $w$  of the Cagliotti formula), one mixing ( $\eta$ ), one asymmetry, two lattice, and two isotropic displacement parameters for InPd<sub>3</sub>. Refined crystal structure data are given in Table 1, Rietveld plots and crystal structure representations in Figs. 1–3 and 4–6, respectively.

Further details of the crystal structure investigations may be obtained from Fachinformationszentrum Karlsruhe,

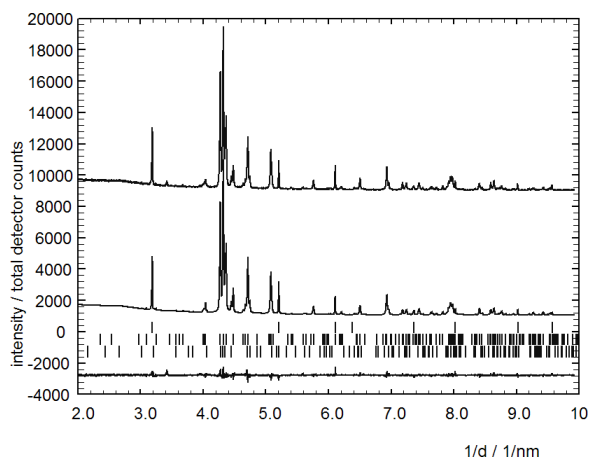


Fig. 1. Observed (top), calculated (middle) and difference (bottom) X-ray powder diffraction patterns of  $\text{In}_3\text{Pd}_5$  at r. t. ( $\text{CuK}\alpha_1$  radiation,  $T = 296(1)$  K, abscissa:  $d^* = 1/d = 2 \sin \theta / \lambda = Q/2\pi$ ). Bragg markers indicate the peak positions of the internal silicon standard (top),  $\text{In}_3\text{Pd}_5$  (middle) and the minor phase  $\text{InPd}_2$  (bottom).

76344 Eggenstein-Leopoldshafen, Germany (Fax: +49-7247-808-666; e-mail: [crysdata@fiz-karlsruhe.de](mailto:crysdata@fiz-karlsruhe.de), [http://www.fizinformationsdienste.de/en/DB/icsd/depot\\_anforderung.html](http://www.fizinformationsdienste.de/en/DB/icsd/depot_anforderung.html)) on quoting the deposition numbers CSD-417906 ( $\text{In}_3\text{Pd}_5$ ), CSD-417907 ( $\text{InPd}_2$ ), and CSD-417908 ( $\text{InPd}_3$ ).

## Results and Discussion

### $\text{In}_3\text{Pd}_5$

$\text{In}_3\text{Pd}_5$  has been reported to crystallize in the orthorhombic  $\text{Rh}_5\text{Ge}_3$  structure, but the standard uncertainties of positional parameters were rather large [34]. Our diffraction data confirm the structure type of  $\text{Rh}_5\text{Ge}_3$  [35], which may be described as a stuffed, distorted variety of the  $\text{CoSn}$ -type [36] or a distorted  $\text{Pt}_5\text{Ga}_3$ -type structure [37]. We provide crystal structure parameters of much better accuracy than reported previously. In2 forms strongly distorted honeycomb nets ( $6^3$  nets) at  $z = 0$  and  $1/2$ , while Pd1 and Pd2 together form Kagomé nets ( $3.6.3.6$  nets) at  $z = 1/4$  and  $3/4$  (Fig. 4). This results in trigonal  $\text{In}_2\text{Pd}_6$  prisms, which are linked by common triangular faces giving infinite columns along the  $c$  axis, and linked by common edges to a three-dimensional framework. Additional indium (In1) and palladium (Pd3) atoms are found within the resulting hexagonal channels, thus completing the coordination sphere of In2 to a total of ten palladium neighbours (In2–Pd distances ranging from 269.0(4) to 297.4(4) pm with a mean dis-

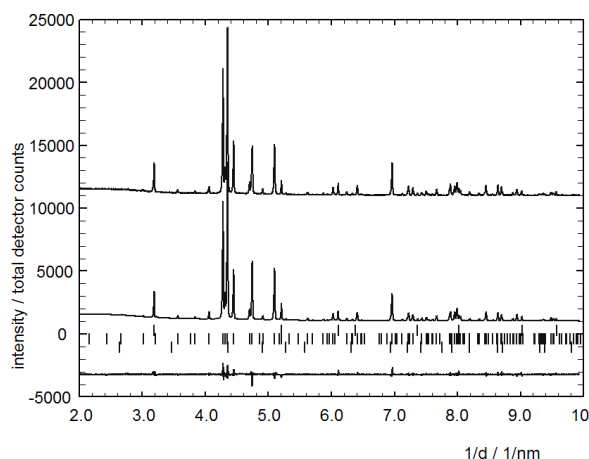


Fig. 2. Observed (top), calculated (middle) and difference (bottom) X-ray powder diffraction patterns of  $\text{InPd}_2$  at r. t. ( $\text{CuK}\alpha_1$  radiation,  $T = 296(1)$  K, abscissa:  $d^* = 1/d = 2 \sin \theta / \lambda = Q/2\pi$ ). Bragg markers indicate the peak positions of the internal silicon standard (top),  $\text{InPd}_2$  (middle) and the minor phase  $\text{InPd}_3$  (bottom).

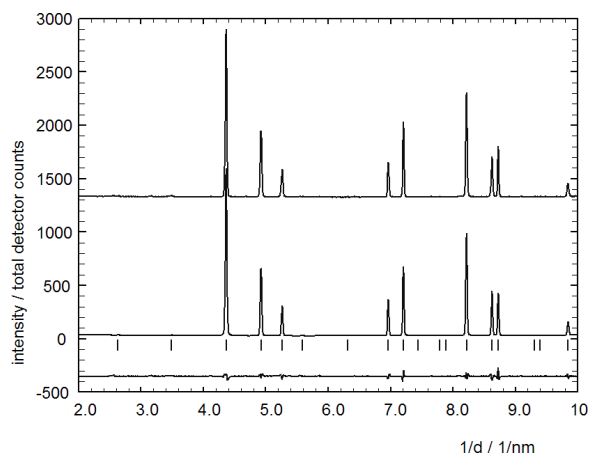


Fig. 3. Observed (top), calculated (middle) and difference (bottom) neutron powder diffraction patterns of  $\text{InPd}_3$  (D1A,  $\lambda = 190.931(3)$  pm,  $T = 299(2)$  K, abscissa:  $d^* = 1/d = 2 \sin \theta / \lambda = Q/2\pi$ ). Bragg markers indicate the peak positions of  $\text{InPd}_3$ .

tance of 281.4 pm) by capping two faces of the prisms by one and the third by two Pd3 atoms. The In1 atoms inside the channels have an eightfold coordination by palladium and are located in the middle of a double prism with the shared prism face lying in the  $ab$  plane (Fig. 4) with In–Pd distances ranging from 267.8(2) to 280.67(2) pm. The somewhat shorter average distance In1–Pd of 272.3 pm reflects the lower coordination number of In1 in comparison to In2.

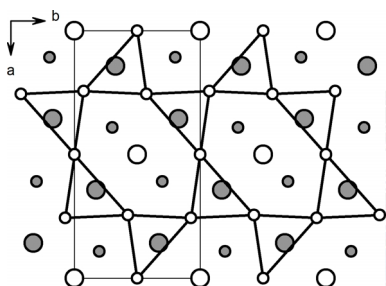


Fig. 4. Projection of the crystal structure of  $\text{In}_3\text{Pd}_5$  in the orthorhombic  $\text{Rh}_5\text{Ge}_3$ -type structure. Large circles represent In, small circles Pd, open circles are located at  $z = 0$ , filled circles at  $z = 1/2$ .

### $\text{InPd}_2$

$\text{InPd}_2$  has been reported in the orthorhombic  $\text{Co}_2\text{Si}$ -type structure, but the crystal structure was not refined in this early work [34]. Our diffraction data confirm that structure type and for the first time provide refined positional parameters (Table 1). Indium is surrounded by ten palladium atoms as tetracapped trigonal prisms (In–Pd distances ranging from 268.9(2) to 291.8(2) pm with an average distance of 278.1 pm). These prisms are linked *via* common triangular faces to form infinite columns along the  $b$  axis and by common corners to form zigzag chains running along  $a$  (Fig. 5). Neighboring chains are shifted by  $1/2 b$ , in such a way that prism atoms in one chain are capping atoms in the neighbouring one and *vice versa*. The lattice parameter ratios  $a/c = 0.683$  and  $(a+c)/b = 3.28$  (Table 1) place  $\text{InPd}_2$  into the  $\text{Co}_2\text{Si}$ -type [38] branch within the  $\text{PbCl}_2$ -type structure family according to [39], which is to be expected because of the rather low ionicity in such intermetallics.

### $\text{InPd}_3$

For  $\text{InPd}_3$  a  $\text{TiAl}_3$ -type structure was proposed on the basis of X-ray powder diffraction data [40]. This structure type represents a superstructure of the cubic closest packing (Cu-type) with identical coordination numbers for all crystallographic sites. Hence, it is lacking a strong crystal chemical differentiation of both elements in contrast to the crystal structures of  $\text{InPd}_2$  and  $\text{In}_3\text{Pd}_5$ , making it more prone to a possible occupational In/Pd disorder and compositional variation. The latter can be confirmed from phase diagrams exhibiting a homogeneity range in  $\text{In}_{1+x}\text{Pd}_{3-x}$  from 24.8 to 26, and at temperatures above 1340 K even up to 27 atomic percent indium [41]. In accor-

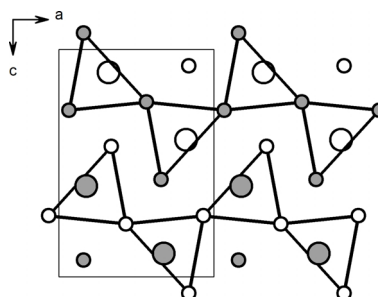


Fig. 5. Projection of the crystal structure of  $\text{InPd}_2$  in the orthorhombic  $\text{Co}_2\text{Si}$ -type structure. Large circles represent In, small circles Pd, open circles are located at  $y = 1/4$ , filled circles at  $y = 3/4$ .

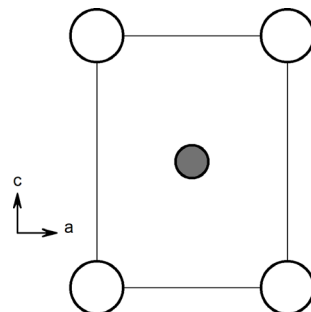


Fig. 6. Projection of the crystal structure of  $\text{InPd}_3$  in the tetragonal  $\text{AuCu}$ -type structure with occupational disorder. Large open circles represent a mixed metal site with 50% In and 50% Pd at the height  $y = 0$ . Small circles represent Pd located at  $y = 1/2$ .

dance with this, we find different unit cell volumes, depending on the synthesis temperature and on the nominal molar ratios of indium and palladium. Unit cell volumes range from  $0.12605(1) \text{ nm}^3$  for the indium-rich to  $0.125474(8) \text{ nm}^3$  for the palladium-rich  $\text{InPd}_3$  phases prepared by the iodine-catalyzed route at 850 K. For quenched samples synthesized at higher temperatures (1450 K) the indium-rich phase boundary extends even further to  $0.126132(5) \text{ nm}^3$ . The synthesis of  $\text{InPd}_3$  from stoichiometric amounts of the elements at lower temperatures (750 K) produced a mixture of two phases  $\text{In}_{1+x}\text{Pd}_{3-x}$  with different cell parameters ( $a = 406.675(4)$ ,  $c = 760.45(2)$  pm and  $a = 410.03(3)$ ,  $c = 747.84(8)$  pm, respectively), one of which is most probably rich in indium ( $x > 0$ ), the other in palladium ( $x < 0$ ).

Unfortunately, indium and palladium are difficult to distinguish by X-rays (49 vs. 46 electrons). Neutrons ( $b_c = 4.1$  vs. 5.9 fm [42]) are much better suited for this task and thus we collected neutron powder diffraction data on  $\text{InPd}_3$  in order to reveal the exact ordering

of In and Pd, which is of importance in view of the hydrogen-induced atomic rearrangement in palladium-rich intermetallics [28]. The neutron powder diffraction data taken on D1A have shown a considerable intensity mismatch with diagrams calculated on the basis of the proposed ordered  $\text{TiAl}_3$ -type structure. Refinement of individual Debye-Waller factors or occupation parameters pointed at a mixed In/Pd occupation of the sites  $2a$  (0, 0, 0) and  $2b$  (0, 0, 1/2) in space group  $I4/mmm$ , while no such indication was found for the site  $4d$  (0, 1/2, 1/4) occupied by palladium. Refinement of occupation parameters lead to values not significantly different from 0.50 for the  $2a$  and  $2d$  sites. Thus lifting the chemical differentiation between those sites, they become crystallographically equivalent, since the whole structure can now be described in the higher symmetric space group  $P4/mmm$  with  $a' = 1/2(a + b)$ ,  $b' = 1/2(-a + b)$ ,  $c' = 1/2c$ . Such a structural model corresponds to an AuCu-type arrangement with mixed In/Pd occupancy on one of the two crystallographic sites. Rietveld refinement of this model resulted in a good fit (Fig. 3, Table 1), indicating the validity of this structural model. Therefore, we describe the crystal structure of  $\text{InPd}_3$  in a partially disordered tetragonal AuCu-type with 50 % In and 50 % Pd on one crystallographic site (Table 1, Fig. 6). This situation may be expressed by a crystal chemical formula  $(\text{In}_{0.5}\text{Pd}_{0.5})\text{Pd} = \text{InPd}_3$ . Each atom in  $\text{InPd}_3$  is surrounded by twelve neighbours in the form of an antioctahedron slightly compressed along the  $c$  axis at distances ranging from 278.14(1) to 287.22(1) pm with an average distance of 281.16 pm. Tribochemical activation did not change the order in  $\text{InPd}_3$  in contrast to  $\text{MgPd}_3$  [28].

In view of this new structural model, the question arises, whether the X-ray diffraction data in the older literature [41] were mistakenly assigned to the  $\text{TiAl}_3$ -type, because the disorder was hidden by the almost equal scattering factors of indium and palladium for

X-rays. Another possibility, however, is that synthesis conditions such as temperature or the presence of mineralizing agents, as, *e. g.*, iodine as applied in this work, do influence the order in  $\text{InPd}_3$ , and the structure described here therefore represents a new modification of  $\text{InPd}_3$ . The existence of a high-temperature modification  $\beta$ - $\text{InPd}_3$  had already been claimed from thermal analysis of the palladium-rich part of the indium-palladium phase diagram, but no structural information has been given [43]. To clarify the question of the number of modifications of  $\text{InPd}_3$  and their atomic order, further neutron diffraction experiments on samples prepared under different conditions will be necessary. Unravelling the inherent disorder in  $\text{InPd}_3$  is of importance for the planned hydrogenation studies, because hydrogen was found to change just this atomic order in  $\text{MPd}_3$  compounds [28].

## Conclusion

An iodine-catalyzed synthesis from the elements at moderate temperatures (850 K) gave access to  $\text{In}_3\text{Pd}_5$ ,  $\text{InPd}_2$  and  $\text{InPd}_3$  in the form of well crystallized powders. The crystal structures of  $\text{In}_3\text{Pd}_5$  and  $\text{InPd}_2$  could be confirmed to belong to the proposed  $\text{Rh}_5\text{Ge}_3$ - and  $\text{Co}_2\text{Si}$ -types, respectively. Rietveld refinements on X-ray powder diffraction patterns have provided the first accurate crystal structure data for these compounds. For  $\text{InPd}_3$  the proposed  $\text{TiAl}_3$ -type structure could be not confirmed, because Rietveld refinement on neutron powder diffraction data revealed an In/Pd distributional disorder. We describe the crystal structure of  $\text{InPd}_3$  in a partially disordered tetragonal AuCu-type with 50 % In and 50 % Pd on one crystallographic site. Mean In–Pd distances range from 272.3 pm for coordination number 8 for indium to 281.2 for coordination number 12.

## Acknowledgement

Help with the synthesis of the  $\text{In}_3\text{Pd}_5$  and  $\text{InPd}_2$  samples by Thorsten Voltmer is highly appreciated.

- 
- [1] H. Wilhelm, *Habilitation Thesis*, University of Geneva, Geneva, **1999**.
- [2] E. Bauer, *Kondo Systems and Heavy Fermions: Transport Phenomena*, in *Encyclopedia of Materials: Science and Technology* (Eds.: K. H. J. Buschow, R. W. Cahn, M. C. Flemings, B. Ilschner, E. J. Kramer, S. Mahajan), Elsevier, Amsterdam, **2001**, p. 4372.
- [3] R. S. Kumar, H. Kohlmann, B. E. Light, A. L. Cornelius, V. Raghavan, T. W. Darling, J. L. Sarrao, *Phys. Rev. B.* **2004**, *69*, 014515.
- [4] K. H. J. Buschow, P. C. P. Bouten, A. R. Miedema, *Rep. Prog. Phys.* **1982**, *45*, 937.
- [5] K. H. J. Buschow, *Hydrogen Absorption in Intermetallic Compounds*, in *Handbook on the Physics and Chemistry of Rare Earths*, Vol. 6 (Eds.: K. A. Gschneidner (Jr.), L. Eyring), Elsevier Science, Amsterdam, **1984**, p. 1.
- [6] B. Chevalier, J.-L. Bobet, E. Gaudin, M. Pasturel, J. Etourneau, *J. Solid State Chem.* **2002**, *168*, 28.

- [7] B. Chevalier, M.L. Kahn, J.-L. Bobet, M. Pasturel, J. Etourneau, *J. Phys.: Condens. Matter* **2002**, *14*, L365.
- [8] B. Chevalier, J.-L. Bobet, M. Pasturel, E. Bauer, F. Weill, R. Decourt, J. Etourneau, *Chem. Mater.* **2003**, *15*, 2181.
- [9] B. Chevalier, J.-L. Bobet, M. Pasturel, E. Gaudin, J. Etourneau, *J. Alloys Compd.* **2003**, *356–357*, 147.
- [10] B. Chevalier, A. Wattiaux, L. Fournès, M. Pasturel, *Solid State Sci.* **2004**, *6*, 573.
- [11] B. Chevalier, M. Pasturel, J.-L. Bobet, R. Decourt, J. Etourneau, O. Isnard, J. Sanchez Marcos, J. Rodriguez Fernandez, *J. Alloys Compd.* **2004**, *383*, 4.
- [12] B. Chevalier, J. Sanchez Marcos, J. Rodriguez Fernandez, M. Pasturel, F. Weill, *Phys. Rev. B.* **2005**, *71*, 214437.
- [13] B. Chevalier, A. Wattiaux, J.-L. Bobet, *J. Phys.: Condens. Matter* **2006**, *18*, 1743.
- [14] B. Chevalier, S.F. Matar, M. Ménétrier, J. Sanchez Marcos, J. Rodriguez Fernandez, *J. Phys.: Condens. Matter* **2006**, *18*, 6045.
- [15] B. Chevalier, C.P. Sebastian, R. Pöttgen, *Solid State Sci.* **2006**, *8*, 1000.
- [16] B. Chevalier, R. Decourt, B. Heying, F.M. Schapacher, U.C. Rodewald, R.-D. Hoffmann, R. Pöttgen, R. Eger, A. Simon, *Chem. Mater.* **2007**, *19*, 28.
- [17] K. Yvon, *Metal Hydrides: Transition Metal Hydride Complexes*, in *Encyclopedia of Materials: Science and Technology* (Eds.: K. H. J. Buschow, R. W. Cahn, M. C. Flemings, B. Ilschner, E. J. Kramer, S. Mahajan), Elsevier, Amsterdam, **2004**, pp. 1–9.
- [18] R. Černý, J.-M. Joubert, H. Kohlmann, K. Yvon, *J. Alloys Compd.* **2002**, *340*, 180.
- [19] W. Bronger, G. Auffermann, *Chem. Mater.* **1998**, *10*, 2723.
- [20] G. Auffermann, W. Bronger, P. Müller, G. Roth, H. Schilder, T. Sommer, *Z. Anorg. Allg. Chem.* **2005**, *631*, 1060.
- [21] H. Kohlmann, R.O. Moyer Jr., T. Hansen, K. Yvon, *J. Solid State Chem.* **2003**, *174*, 35.
- [22] R.O. Moyer Jr., B.H. Toby, *J. Alloys Compd.* **2004**, *363*, 99.
- [23] W. Bronger, K. Jansen, P. Müller, *J. Less-Common Met.* **1990**, *161*, 299.
- [24] E. Rönnebro, D. Noréus, M. Gupta, K. Kadir, B. Hauback, P. Lundqvist, *Mater. Res. Bull.* **2000**, *35*, 315.
- [25] W. Bronger, G. Ridder, *J. Alloys Compd.* **1994**, *210*, 53.
- [26] M. Olofsson-Martenson, M. Kritikos, D. Noreus, *J. Am. Chem. Soc.* **1999**, *121*, 10908.
- [27] H. Kohlmann, H.E. Fischer, K. Yvon, *Inorg. Chem.* **2001**, *40*, 2608.
- [28] H. Kohlmann, G. Renaudin, K. Yvon, C. Wannek, B. Harbrecht, *J. Solid State Chem.* **2005**, *178*, 1292.
- [29] C. Wannek, B. Harbrecht, *Z. Anorg. Allg. Chem.* **2000**, *626*, 1540.
- [30] C. Wannek, B. Harbrecht, *J. Solid State Chem.* **2001**, *159*, 113.
- [31] C. Wannek, B. Harbrecht, *J. Alloys Compd.* **2001**, *316*, 99.
- [32] C. Wannek, B. Harbrecht, *Z. Anorg. Allg. Chem.* **2002**, *628*, 1597.
- [33] J. Rodriguez-Carvajal, FULLPROF.2K (version 3.70), A Program for Rietveld Refinement and Pattern Matching Analysis, Jul2006-ILL JRC, **2006**, unpublished. See also: *Physica B*, **1993**, *192*, 55–69, Satellite Meeting on Powder Diffraction of the 15<sup>th</sup> International Congress of the IUCr, Toulouse (France) **1990**, p. 127.
- [34] K. Schubert, H.L. Lukas, H.-G. Meißner, S. Bhan, *Z. Metallkd.* **1959**, *50*, 534.
- [35] S. Geller, *Acta Crystallogr.* **1955**, *8*, 15.
- [36] H. Bärmighausen, *MATCH Comm. Math. Chem.* **1980**, *9*, 139.
- [37] H. Kohlmann, H.P. Beck, *Z. Anorg. Allg. Chem.* **1997**, *623*, 785.
- [38] S. Geller, V.M. Wolontis, *Acta Crystallogr.* **1955**, *8*, 83.
- [39] W. Jeitschko, *Acta Crystallogr. B* **1968**, *24*, 930.
- [40] S. Bhan, K. Schubert, *J. Less-Common Met.* **1969**, *17*, 73.
- [41] J.R. Knight, D.W. Rhys, *J. Less-Common Met.* **1959**, *1*, 292.
- [42] V.F. Sears, *Neutron News* **1992**, *3*, 26.
- [43] E.E. Schmid, V. Carle, *Prakt. Metallogr.* **1988**, *25*, 340.